Journal of Molecular Structure 1223 (2020) 128973

Contents lists available at ScienceDirect

Journal of Molecular Structure

journal homepage: www.elsevier.com/locate/molstr

Identifying and explaining the regioselectivity of alkylation of 1,2,4-triazole-3-thiones using NMR, GIAO and DFT methods

Maksym Fizer*, Mikhailo Slivka, Nataliya Korol, Oksana Fizer

Department of Organic chemistry, Faculty of chemistry, Uzhhorod national university, Pidgirna Str. 46, 88000 Uzhgorod, Ukraine

ARTICLE INFO

Article history:
Received 17 June 2020
Revised 10 July 2020
Accepted 24 July 2020
Available online 25 July 2020

Keywords:
Alkylation
Electron localization function
Fukui function
GIAO
Regioselectivity
Triazole

ABSTRACT

The regioselectivity of the alkylation of four 1,2,4-triazole-3-thiones with eight different organic halides was determined by the comparison of experimentally observed NMR chemical shifts of the product molecules to those predicted by density functional theory (DFT) calculations via gage independent atomic orbital (GIAO) method. The combination of the employed reactants resulted in ten different model alkylated triazoles, seven of which are new and not previously described. The reaction was performed in neutral and alkaline medium with the observation that S-alkylation occurs selectively and with slightly lower yields under neutral conditions. Highest occupied molecular orbitals, electron localization function, electrophilic Fukui function, and different types of partial charges were considered as reactivity descriptors to reveal the observed regioselectivity and to explain the structure of synthesized products. In conclusion, the comparison of the chemical shifts of ^{1}H and ^{13}C NMR of the α-methylene group of the products with those calculated by incorporating the GIAO DFT-computed isotropic chemical shielding gives an approach for the correct and reliable determination of the site of alkylation as the S-atom of the synthesized S-alkylated 1,2,4-triazoles.

1. Introduction

S- and N-alkylated 1,2,4-triazole-containing systems have become increasingly interesting due to their pharmacological potential. Two widely used medical drugs, namely lesinurad [1] and thiotriazolinone [2] contain a carboxymethylsulfonyl fragment, and are synthetically available through the S-alkylation of corresponding 1,2,4-triazole-3-thiones.

In recognition of the relationship of structure and pharmacological action, the determination of the molecular structure of azoles is an important subject of organic chemistry. The search for new methods for the derivatization of 1,2,4-triazole-containing systems via the alkylation reaction, as well as reliable routes to solve their structure are important tasks due to the increasing interest in the obtained S(N)-alkylated products and the possibility for their further transformation [3–6].

The most recent approaches of S-alkylation of 1,2,4-triazole-3-thiol are described as the interaction between the mentioned heterocyclic system and corresponding alkylating agents: alkyl/alkenyl/alkynyl/benzyl halides [3–8], halogen-substituted carboxylic acids [9–11], halogenacetamides [10,11], haloalkanoic acid esters [10–12] and chloroacetophenones [13]. The alkylation protocols differ in the solvents (alcohol, acetone, water) and bases (KOH, K_2CO_3, pyridine) used and influence the regioselectivity in the performed reactions. In most cases, 1,2,4-triazole thioethers will be obtained as target products if the sulfur atom is not yet alkylated [4–8]. However, together with the formation of S-alkylated product some authors described the formation of N-alkylated derivatives as well. Thus, Samvelyan et al. [12] described that alkylation of S-unprotected 1,2,4-triazole-3-thiol with methyl 3-bromopropanoate gave an inseparable mixture of S- and 2-N-alkylation products. According to Boraei et al. [7] the 2-N-allylated product was obtained after fusing of allylsulfanyl-4-amino-1,2,4-triazole in the absence of either solvent or catalyst. The alkylation of S-substituted 1,2,4-triazoles in the presence of K_2CO_3 gave a mixture of two products of which the S-, 2-N-alkylated triazole was formed in higher yields than S-, 1-N-alkylated triazoles [8].

Investigations on some biological properties of S-(N)-alkylated 1,2,4-triazole-3-thiols were also reported [6,10,11,13]. The antiproliferative assay against hepatic and breast cancer cell lines preliminary showed promising antitumor activity of S- and 1-N-alkylated derivatives of 1,2,4-triazole-3-thiol compared to the standard drug, doxorubicin [6]. The results of the effects of the compounds on the DNA methylation level revealed that S-alkylated analogues possessed a greater demethylating activity compared to the low activity of 1-N-substituted compounds [10]. According to preliminary screening results, five of the six tested S-alkylated compounds ex-

* Corresponding author.
E-mail address: max.fizer@uzhnu.edu.ua (M. Fizer).

https://doi.org/10.1016/j.molstruc.2020.128973
0022-2860/

hibited antiulcer activity at the level of the reference drug ranitidine [13]. S-alkylated triazoles also showed a moderate to good activity against gram-positive (*Bacillus cereus, Staphylococcus aureus*) and gram-negative (*Escherichia coli, Pseudomonas aeruginosa*) bacteria [11].

NMR technique is one of the most powerful methods for resolving the molecular structure of organic compounds and may be successfully used for the investigation of the spatial structure of peptides [14], for studying small organic guest molecules physisorbed on different mesoporous silicas [15], for the exploration of functionalized N-phenylbenzamides [16], and for enantiomer discrimination of cathinones [17]. Moreover, combined NMR and DFT GIAO investigations were performed for the determination of structures of galantamine derivatives [18] and organosulfur compounds [19]. Such combined studies have also been carried out for compounds containing the 1,2,4-triazole ring [20,21].

A description of various methods for the prediction of NMR parameters is given by Toukach and Ananikov [22]. Among many available methods, the theoretical approaches based on the DFT calculations might be considered as the most affordable and accurate, especially in cases of new systems for which methods that use structure-based parameters can be applied only with limited accuracy due to the absence of appropriate parameterization. One of the most routinely used methods to calculate chemical shifts is the gage independent atomic orbital (GIAO) method [23], which is satisfactory in the prediction of chemical shifts values due to the adequate calculation of isotropic chemical shielding for different nuclei [24–26].

In the present investigation, the DFT computed ^{1}H, and ^{13}C chemical shifts of various possible isomers of alkylated 1,2,4-triazole-3-thiones are compared with experimental values to reliably determine the structure of the obtained alkylated products and to understand the regioselectivity of the performed alkylation reactions. The numerous reactivity descriptors, namely HOMO, electron localization function, electrophilic Fukui function, and various atomic partial charges have been computed to explain the selectivity of the electrophilic attack on the 1,2,4-triazole-3-thione system. In the course of the investigation, the inclusion of ^{13}C NMR analysis was found necessary for the correct resolving of the structure of the alkylated products.

2. Experimental

The melting points were measured on the Stuart SMP30 instrument. Elemental composition determination was performed on Elementar Vario MICRO cube. ^{1}H NMR (400 MHz) and ^{13}C NMR (100 MHz) spectra were recorded on Varian VXR 400. Samples were studied in deuterated dimethylsulfoxide (DMSO) solutions. Tetramethylsilane was used as a standard in both experimental and computational studies.

2.1. Synthesis

The synthetic procedures for the starting materials, 4-allyl-5-allylamino-2,4-dihydro-*3H*-1,2,4-triazole-3-thione **a** [27], 4-phenyl-5-phenylamino-2,4-dihydro-*3H*-1,2,4-triazole-3-thione **b** [28], 4-phenyl-5-amino-2,4-dihydro-*3H*-1,2,4-triazole-3-thione **c** [29], and 4,5-diphenyl-2,4-dihydro-*3H*-1,2,4-triazole-3-thione **d** [30] are described in the corresponding literature.

Different halogen-containing hydrocarbons were used as alkylation agents in this study, namely: benzyl chloride (α-chlorotoluene, CAS# 100–44–7), propargyl bromide (3–bromo-1-propyne, CAS# 106–96–7), allyl bromide (3–bromo-1-propene, CAS# 106–95–6), cinnamyl chloride ((3-chloropropenyl)benzene, CAS# 2687–12–9), methyl iodide (iodomethane, CAS# 74–88–4), methallylchloride (3–chloro–2-methyl-1-propene, CAS# 563–47–3), crotonylbromide (*trans*-1–bromo-2-butene, CAS# 29,576–14–5), and 4–bromo-1-butene (CAS# 5162–44–7). All used reagents were purchased from commercial suppliers and were of "reagent grade" purity.

General alkylation of 1,2,4-triazole-3-thione. Method 1

4,5-Disubstituted-2,4-dihydro-*3H*-1,2,4-triazole-3-thione **a-d** (10.0 mmol) and potassium hydroxide (12.0 mmol) were added to 20 mL ethanol and heated to give a clear solution. The halogen-containing alkylation agent (12.0 mmol) was added in 5 mL ethanol to the cooled solution of the triazole. The mixture was refluxed for 1–2 h. After cooling, the precipitated product was filtered, washed with deionized water and dried in vacuo. In the case of a small quantity of the precipitated product, the solvent was removed under reduced pressure to form the target precipitate. Substances were purified by crystallization from ethanol.

General alkylation of 1,2,4-triazole-3-thione. Method 2

4,5-Disubstituted-2,4-dihydro-*3H*-1,2,4-triazole-3-thione **a-c** (10.0 mmol) and halogen-containing alkylation agent (12.0 mmol) were added to 50 mL ethanol, and the reaction mixture was refluxed for 3 h. After cooling, a solution of potassium hydroxide (30.0 mmol) in 30 ml water was added to the homogenous reaction mixture which caused the immediate precipitation of the target product **3**. The precipitate was filtered, washed with deionized water, and finally recrystallized from ethanol to obtain the pure substance.

5-(Benzylsulfanyl)-N,4-diallyl-4H-1,2,4-triazol-3-amine (**3a**).

Synthesized from 4-allyl-5-allylamino-4*H*-1,2,4-triazol-3-thione **a** and benzyl chloride. White powder with mp 127–128 °C (from ethanol). The yield is 2.69 g (94%) and 2.32 g (81%) according to method 1 and method 2, respectively. The elemental analysis: found: C, 63.1; H, 6.6; N, 19.5; S 11.0%; calc. for $C_{15}H_{18}N_4S$: C, 62.9; H, 6.3; N, 19.6; S, 11.2%.

^{1}H NMR (400 MHz, DMSO–d6) δ (ppm): 7.25–7.37 (m, 5H, C_6H_5), 6.50 (t, 1H, J = 6.2 Hz, NH), 5.75–5.90 (m, 2H, 2-CH=), 5.05–5.29 (ddd, 4H, J = 54.0, 41.4, 17.2 Hz, $2CH_2$=), 4.65 (d, 2H, J = 3.3 Hz, $C\underline{H}_2$NH-), 4.39 (s, 2H, SCH_2), 4.05 (s, 2H, $CH_2N_{triazole}$).

^{13}C NMR (125 MHz, DMSO–d6) δ (ppm): 152.3, 146.0, 136.6, 133.4, 130.6, 129.5, 129.0, 128.2, 118.7, 117.0, 45.7, 45.2, 37.0.

5-(Benzylsulfanyl)-N,4-diphenyl-4H-1,2,4-triazol-3-amine (**3b**)

Synthesized from 4-phenyl-5-phenylamino-4*H*-1,2,4-triazol-3-thione **b** and benzyl chloride. White powder with mp 207–208 °C (from ethanol). The yield is 3.44 g (96%) and 3.26 g (91%) according to method 1 and method 2, respectively. The elemental analysis: found: C, 70.3; H, 5.4; N, 15.4; S 8.8%; calc. for $C_{21}H_{18}N_4S$: C, 70.4; H, 5.1; N, 15.6; S, 9.0%.

^{1}H NMR (400 MHz, DMSO–d6) δ (ppm): 8.28 (s, 1H, NH), 6.85–7.53 (m, 15H, $3C_6H_5$), 4.22 (s, 2H, SCH_2).

^{13}C NMR (125 MHz, DMSO–d6) δ (ppm): 152.5, 145.9, 141.8, 137.5, 132.7, 130.2, 129.4, 129.0, 128.9, 128.3, 127.8, 120.9, 117.3, 37.2.

N,4-Diphenyl-5-(propargylsulfanyl)−4H-1,2,4-triazol-3-amine (**3c**)

Synthesized from 4-phenyl-5-phenylamino-4*H*-1,2,4-triazol-3-thione **b** and propargyl bromide. White powder with mp 181 °C (from ethanol). The yield is 2.57 g (84%) according to method 1. The elemental analysis: found: C, 66.7; H, 4.9; N, 18.0; S 10.2%; calc. for $C_{17}H_{14}N_4S$: C, 66.6; H, 4.6; N, 18.3; S, 10.5%.

^{1}H NMR (400 MHz, DMSO–d6) δ (ppm): 8.36 (s, 1H, NH), 6.85–7.58 (m, 10H, $2C_6H_5$), 3.79 (s, 2H, SCH_2), 3.31 (s, 1H, HC≡C).

^{13}C NMR (125 MHz, DMSO–d6) δ (ppm): 152.8, 144.8, 141.7, 132.7, 130.3, 129.0, 128.4, 121.0, 117.5, 79.8, 75.2, 21.7.

5-(Allylsulfanyl)-N,4-diphenyl-4H-1,2,4-triazol-3-amine (**3d**)

Synthesized from 4-phenyl-5-phenylamino-4*H*-1,2,4-triazol-3-thione **b** and allylbromide. White powder with mp166–167 °C (from ethanol). The yield is 2.74 g (89%) according to method 1. The elemental analysis: found: C, 66.4; H, 5.5; N, 18.1; S 10.2%; calc. for $C_{17}H_{16}N_4S$: C, 66.2; H, 5.2; N, 18.2; S, 10.4%.

^{1}H NMR (400 MHz, DMSO–d6) δ (ppm): 8.26 (s, 1H, NH), 6.56–7.80 (m, 10H, $2C_6H_5$), 5.58–6.04 (m, 1H, -CH=), 5.08 (dd, 2H, J = 38.3, 13.3 Hz, CH_2=), 3.56 (d, 2H, J = 5.9 Hz).

^{13}C NMR (125 MHz, DMSO–d6) δ (ppm): 152.5, 145.5, 141.8, 133.8, 132.8, 130.3, 129.0, 128.4, 120.9, 118.8, 117.3, 35.7.

5-(Methylsulfanyl)-N,4-diphenyl-4H-1,2,4-triazol-3-amine (**3e**)

Synthesized from 4-phenyl-5-phenylamino-4*H*-1,2,4-triazol-3-thione **b** and methyl iodide. White powder with mp 224–226 °C (from ethanol), lit. 225–229 °C [31]. The yield is 2.60 g (92%) according to method 1. The elemental analysis: found: C, 63.7; H, 5.1; N, 19.8; S 11.3%; calc. for $C_{15}H_{14}N_4S$: C, 63.8; H, 5.0; N, 19.8; S, 11.4%.

^{1}H NMR (400 MHz, DMSO–d6) δ (ppm): 8.33 (s, 1H, NH), 6.84–7.58 (m, 10H, $2C_6H_5$), 2.50 (s, 3H, SCH_3).

^{13}C NMR (100 MHz, DMSO–d6) δ (ppm): 152.5, 147.5, 142.0, 132.8, 130.4, 130.3, 129.1, 128.2, 120.9, 117.3, 14.9.

5-(Cinnamylsulfanyl)-N,4-diphenyl-4H-1,2,4-triazol-3-amine (**3f**)

Synthesized from 4-phenyl-5-phenylamino-4*H*-1,2,4-triazol-3-thione **b** and cinnamyl chloride. White powder with mp 200–201 °C (decompose) (from ethanol). The yield is 3.65 g (95%) and 3.15 g (82%) according to method 1 and method 2, respectively. The elemental analysis: found: C, 72.1; H, 5.5; N, 14.4; S 8.1%; calc. for $C_{23}H_{20}N_4S$: C, 71.9; H, 5.2; N, 14.6; S, 8.3%.

^{1}H NMR (400 MHz, DMSO–d6) δ (ppm): 8.22 (s, 1H, NH), 6.82–7.55 (m, 15H, $3C_6H_5$), 6.51 (d, 1H, J = 15.7 Hz, Ph–C<u>H</u>=), 6.16–6.33 (m, 1H, =C<u>H</u>–CH_2S), 3.79 (d, 2H, J = 7.0 Hz, SCH_2).

^{13}C NMR (125 MHz, DMSO–d6) δ (ppm): 152.6, 145.8, 141.9, 136.7, 133.3, 132.9, 130.2, 130.2, 129.1, 129.1, 128.5, 128.3, 126.8, 125.2, 120.9, 117.4, 36.0.

5-(Methallylsulfanyl)-N,4-diphenyl-4H-1,2,4-triazol-3-amine (3 g)

Synthesized from 4-phenyl-5-phenylamino-4*H*-1,2,4-triazol-3-thione **b** and methallyl chloride. White powder with mp 192–194 °C (from ethanol). The yield is 2.90 g (90%) according to method 1. The elemental analysis: found: C, 67.3; H, 5.9; N, 17.4; S 9.6%; calc. for $C_{18}H_{18}N_4S$: C, 67.1; H, 5.6; N, 17.4; S, 9.9%.

^{1}H NMR (400 MHz, DMSO–d6) δ (ppm): 8.15 (s, 1H, NH), 6.65–7.77 (m, 10H, $2C_6H_5$), 4.81 (d, 2H, J = 13.8 Hz, CH_2=), 3.56 (s, 2H, CH_2S), 1.67 (s, 3H, CH_3).

^{13}C NMR (125 MHz, DMSO–d6) δ (ppm): 152.6, 145.6, 141.9, 140.8, 132.9, 130.3, 130.2, 129.1, 128.5, 121.0, 117.4, 115.1, 40.7, 21.1.

5-(Methylsulfanyl)−4-phenyl-4H-1,2,4-triazol-3-amine (3 h)

Synthesized from 4-phenyl-4*H*-1,2,4-triazol-3-thione **c** and methyl iodide. White powder with mp 144–146 °C (from ethanol). The yield is 2.90 g (90%) according to method 1. The elemental analysis: found: C, 54.6; H, 5.8; N, 25.2; S 14.3%; calc. for $C_{10}H_{12}N_4S$: C, 54.5; H, 5.5; N, 25.4; S, 14.6%.

^{1}H NMR (400 MHz, DMSO–d6) δ (ppm): 7.35–7.57 (m, 5H, C_6H_5), 5.71 (s, 2H, NH_2), 2.38 (s, 3H, SCH_3).

^{13}C NMR (100 MHz, DMSO–d6) δ (ppm): 156.3, 144.8, 133.2, 130.3, 129.8, 127.8, 15.5.

3-{[(2E)-B*ut*-2-*en*-1-*yl*]sulfanyl}−4,5-diphenyl-4H-1,2,4-triazole (**3i**)

Synthesized from 4,5-diphenyl-4*H*-1,2,4-triazol-3-thione **d** and (2E)−1-bromobut-2-ene. White powder with mp 137–139 °C (from ethanol), lit. 137–139 °C [6]. The yield is 2.82 g (92%) according to method 1. The elemental analysis: found: C, 70.5; H, 5.9; N, 13.6; S 10.2%; calc. for $C_{18}H_{17}N_3S$: C, 70.3; H, 5.6; N, 13.7; S, 10.4%.

^{1}H NMR (400 MHz, DMSO–d6) δ (ppm): 7.29–7.60 (m, 10H, $2C_6H_5$), 5.64–5.70 (m, 1H, –CH=), 5.43–5.59 (m, 1H, –CH=), 3.77 (dd, 2H, J = 28.6, 7.1 Hz, SCH_2), 1.61 (s, 3H, CH_3).

^{13}C NMR (100 MHz, DMSO–d6) δ (ppm): 154.7, 151.9, 134.3, 130.4, 130.1, 129.8, 129.2, 129.0, 128.8, 128.2, 127.1, 126.2, 34.8, 18.0.

*3-[(But-3-en-1-yl)sulfanyl]−4,5-diphenyl-4H-1,2,4-triazole (**3j**)*

Synthesized from 4,5-diphenyl-4*H*-1,2,4-triazol-3-thione **d** and 4–bromo-1-butene. White powder with mp133–135 °C (from ethanol), lit. 133–135 °C [6]. The yield is 2.86 g (93%) according to method 1. The elemental analysis: found: C, 70.2; H, 5.8; N, 13.4; S 10.1%; calc. for $C_{18}H_{17}N_3S$: C, 70.3; H, 5.6; N, 13.7; S, 10.4%.

^{1}H NMR (400 MHz, DMSO–d6) δ (ppm): 7.44–7.58 (m, 10H, $2C_6H_5$), 5.79 (m, 1H, –CH=), 4.98–5.14 (m, 2H, =CH_2), 3.22 (t, 2H, J = 7.2 Hz, SCH_2), 2.45 (d, 2H, J = 7.1, CH_2).

^{13}C NMR (100 MHz, DMSO–d6) δ (ppm): 154.8, 152.3, 136.6, 134.4, 130.5, 130.4, 130.2, 129.0, 128.3, 128.2, 127.1, 117.1, 33.5, 31.7.

2.2. Computational methods

The choice of the energetically preferred rotamers of all studied compounds, except those resolved with the XRD technique, was based on conformers' search through the systematic rotor engine in the Avogadro [32] program. The MMFF94 force field [33] was applied in these calculations. Then, the most stable rotamer was re-optimized with DFT method.

The gas phase geometry optimizations were performed at the PBE/6–31G(d) level in the PRIRODA program [34–36]. Geometry optimization was followed by a Hessian calculation to verify that the obtained geometries correspond to the true energy minima, as there were no imaginary frequencies present.

The GIAO approach was used to calculate the NMR chemical shifts using the PBE/6–31G(d) and PBE/λ3 methods [37] in the PRIRODA program and with the B3LYP/6–31G(d) and B3LYP/6–31G(d,p) methods [38] in the ORCA 4.2.1 program [39]. In case of the PBE functional, gas phase NMR calculations were performed, whereas in the case of GIAO-B3LYP calculations, the DMSO solvent influence was modelled via the CPCM solvation model [40].

Because the PBE0 hybrid functional is known to be suitable for the modeling of electron densities [41,42], the electron density of the starting substrate species was calculated at the PBE0/6–311++G(d,p) level of theory. Electrophilic Fukui functions [43], as well as electron localization functions [44] were generated with the Multiwfn 3.6 program [45]. The capability of the correct regioselectivity prediction was calculated for numerous types of partial charges, namely: Mulliken [46], Löwdin [47], CHELPG [48], and Hirshfeld [49] partial charges were computed in the ORCA program, whereas the extensions of Hishfeld population analysis, like CM5 [50] and ADCH [51] partial charges were calculated in CM5charges [52] and in Multiwfn programs, respectively. Natural population analysis [53] and calculation of respective partial charges have been carried out in JANPA code [54]. Visualization of structures and isosurfaces, as well as figures rendering was accomplished using the UCSF Chimera software [55]. Density fitting [56] and resolution of identity with chain-of-spheres techniques [57,58] were enabled where possible to speed-up the calculations.

3. Results and discussion

3.1. Synthesis and NMR study

Alkylation was performed in two principally different manners. In the first method, the thiones **a-d** were dissolved in alkaline medium, which causes a proton elimination from the nitrogen in 2-position of the triazole ring with further transformation into thiolate anion (Scheme 1) as the nucleophilic reactant for the subsequent alkylation step. In the second method, the alkylation agent reacts with the neutral 1,2,4-triazole species, which, due to tautomerism, can exist as a mixture of the thione and thiol form, whereby the thione form exhibits a higher stability than the thiol form in neutral medium according to numerous theoretical and experimental works [59–62]. The hydrogen halide, which was formed

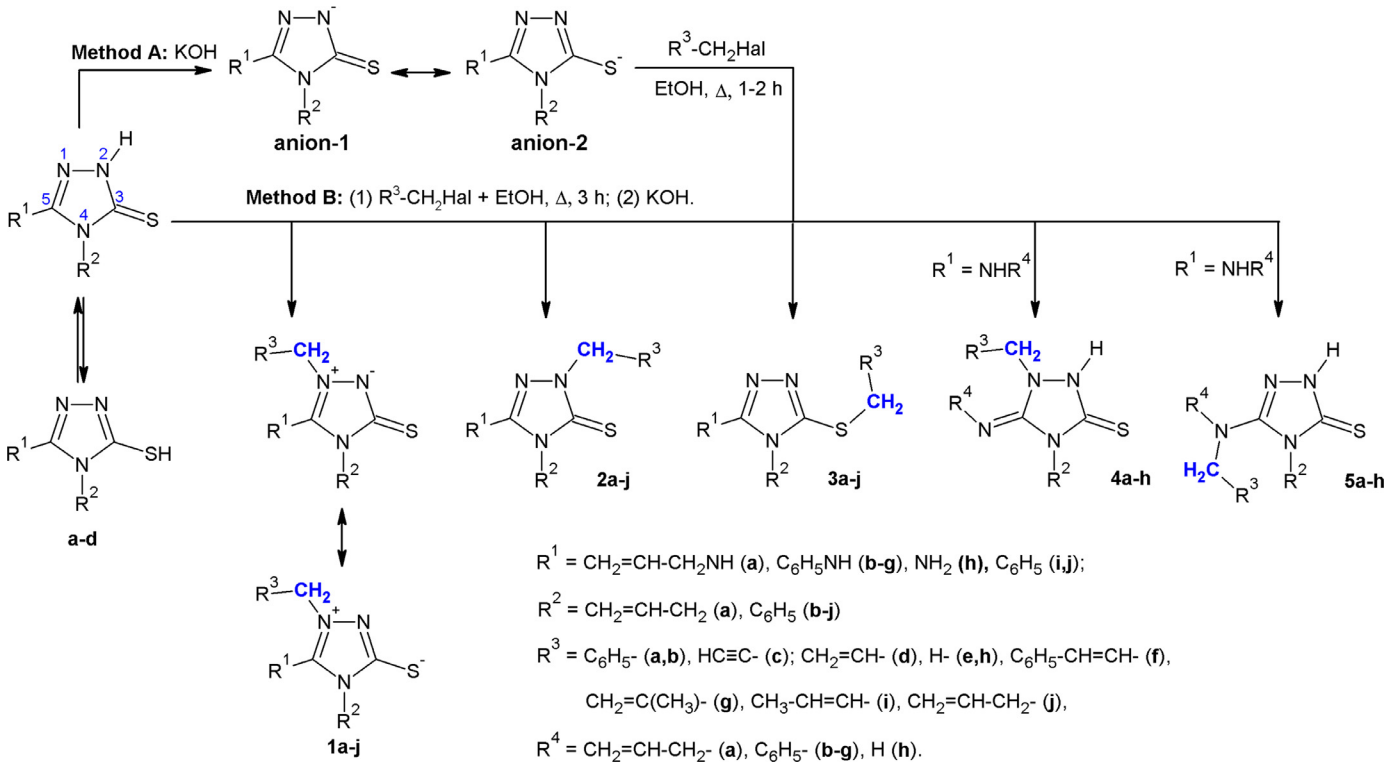

Scheme 1. Alkylation of model thiones **a-d** with all possible alternative products.

during the alkylation reaction, was then neutralized with potassium hydroxide in the next step.

In theory, alkylation can take place at different reaction centers of the model 1,2,4-triazole-3-thions **a-d** (see Scheme 1). In the case of alkylation of the nitrogen in 1-position of the triazole ring, the zwitterionic structures **1a-j** can be formed. In addition, 5-R-amino substituted triazole-3-thiones **a-c** can react to the alternative structures **4a-h** because of the existing tautomerization in the guanidine fragment. Due to the two anionic mesomeric structures of triazole-1-ide (**anion-1**) and triazole-3-thiolate (**anion-2**), the electrophilic attack of alkyl halides can lead to the formation of compounds **2a-j** or **3a-j**, respectively. Finally, the presence of the exocyclic NH-fragment bound to the 5-position of the triazole ring, unlocks the possibility of attachment of the alkyl group to the exocyclic nitrogen and formation of structures **5a-h**.

While acknowledging the possible thione-thiol tautomerism for the structures **4a-h** and **5a-h**, due to lower stability of thiols, only thionic forms were considered in the NMR calculations.

To correctly resolve the structure of the obtained products, and to determine the regiodirection of the alkylation reaction, the ^{1}H and ^{13}C spectra were recorded. For the assignment of the experimentally observed peaks, it was decided to compare these with GIAO DFT-based calculated NMR chemical shifts of all proposed alternative structures **1–5**. During analysis of the experimental and theoretical NMR spectra, we have focused mainly on the signals of the α-methylene, or methyl in the case of methyl iodide as the alkylating agent. These groups are highlighted in blue in Scheme 1.

As the first step, a geometry optimization of all proposed structures was carried out. For geometry optimization and related vibrational frequencies calculations, the GGA PBE functional was used, which gave relatively good performance/accuracy ratio in our previous works [63–65]. Here we also have to mention a good performance of PBE functional for distinguishing conformers' relative stability [66,67]. Considering that 46 possible products and 12 structures of the triazole substrates (three for each triazole **a-d**) needed to be optimized, the smallest possible but still sufficiently accurate basis set was used. Therefore, we have benchmarked triple-zeta 6–311G(d,p) and double-zeta 6–31G(d), 6–31G(d,p) and 6–31+G(d,p) basis sets over two triazole structures resolved with single crystal X-ray diffraction. The 4-phenyl-5-phenylamino-1,2,4-triazole-3-thione [28], which is marked as thione **b** in this study, and 3-(methylsulfanyl)−4-phenyl-5-(phenylamino)−*4H*-1,2,4-triazole-1-ium cation, which is protonated form of structure **3e**, as its hexabromotellurate salt [31], were used as the reference structures.

The correlation between PBE DFT calculated and experimental values of interatomic distances and bond angles is shown in Table 1. For the calculated interatomic distances, in the case of the gas-phase calculations, the correlation coefficient, R^2, systematically marginally increases and equals 0.9553, 0.9557, 0.9571, 0.9586 for the tested 6–31G(d), 6–31G(d,p), 6–31+G(d,p), 6–311G(d,p) basis set, respectively. An analogous increase of R^2 can be observed in the case of the implicit CPCM solvation model. A similar observation is made for the bond angles, where in the case of gas-phase computations, the correlation coefficients equal 0.9658, 0.9660, 0.9663, and 0.9688 for the 6–31G(d), 6–31G(d,p), 6–31+G(d,p), 6–311G(d,p) basis sets, respectively. It must be noticed the slight systematic increase of R^2 in the case of CPCM interatomic distances in comparison to the gas-phase data. Oppositely, in the case of bond angles, the correlation coefficient is higher for the gas-phase calculations.

As a result, only marginal improvement of bond length and bond angles can be obtained through shifting from the double-zeta 6–31G(d) basis set to more computationally expensive basis sets. Although the use of the CPCM solvation model leads to an improvement of interatomic distances, it simultaneously entails deterioration of bond angles values and is more time-consuming, especially for calculation of Hessian. For this reason, the optimization of all geometries was done in a gas phase with more computationally affordable 6–31G(d) basis set. Moreover, using gas-phase geome-

Table 1
Comparison of PBE DFT calculated and XRD experimental geometrical parameters: interatomic distances and bond angles. S – slope, I – intercept, R^2 – correlation coefficient.

Correlation between geometries	Basis set	Interatomic distances			Bond angles		
		S	I	R^2	S	I	R^2
XRD and Gas phase	6–31G(d)	1.0333	−0.0740	0.9553	0.9571	4.9703	0.9658
	6–31G(d,p)	1.0342	−0.0750	0.9557	0.9583	4.8275	0.9660
	6–31+G(d,p)	1.0386	−0.0828	0.9571	0.9633	4.2268	0.9663
	6–311G(d,p)	1.0286	−0.0648	0.9586	0.9642	4.1210	0.9688
XRD and CPCM DMSO	6–31G(d)	1.0006	−0.0279	0.9603	0.9567	5.0039	0.9647
	6–31G(d,p)	1.0012	−0.0286	0.9605	0.9575	4.9103	0.9646
	6–31+G(d,p)	1.0059	−0.0361	0.9607	0.9570	4.9580	0.9619
	6–311G(d,p)	1.0008	−0.0273	0.9620	0.9552	5.1725	0.9632
Gas phase and CPCM DMSO	6–31G(d)	0.9644	0.0502	0.9970	0.9976	0.2700	0.9949
	6–31G(d,p)	0.9642	0.0504	0.9969	0.9973	0.3009	0.9950
	6–31+G(d,p)	0.9652	0.0496	0.9971	0.9926	0.8600	0.9938
	6–311G(d,p)	0.9693	0.0416	0.9961	0.9897	1.2097	0.9922

tries computed at a lower level of theory for further calculation NMR chemical shifts at a higher level is a well-validated strategy [68–71].

Isotropic chemical shielding values were calculated at different levels of theory to determine which level can be routinely used for resolving triazole structures. Gas-phase calculations with PBE functional were performed in combination with a minimal 6–31G(d) basis set and a large quadruple-zeta basis set λ3, which is analog to the cc-pVQZ basis. Since in the PRIRODA quantum chemistry code, calculations with the PBE functional are extremely fast, this method is computationally attractive even in combination with relatively heavy basis sets. Moreover, it was shown that gas-phase PBE calculations can be accurate in GIAO modeling of ^{1}H and ^{13}C NMR chemical shifts [72,73]. It is worth mentioning that in the case of the presence of solute-solvent strong hydrogen bonds, the inclusion of explicit solvent molecules is essential [12,74,75]. However, this is beyond the scope of the present work, and only the implicit solvent model was applied.

B3LYP calculations were combined with 6–31G(d) and 6–31G(d,p) basis sets. The CPCM implicit solvation model was enabled for the inclusion of the DMSO solvent effects. The choice of hybrid B3LYP functional was influenced by previous investigations, where authors found a good prediction capability of this method for triazole systems [21]. In addition, it was demonstrated that hybrid functionals even when combined with relatively small basis sets like 6–31G(d,p) or with lighter 6–31G(d) may provide superior correlation between experimental and GIAO computed ^{1}H NMR isotropic chemical shielding [76].

The comparison of experimentally observed and computed ^{1}H NMR chemical shifts is summarized in Table 2. A direct comparison of linear correlation between the experimental and computed values in terms of correlation coefficient R^2, slope, and intercept would be the wrong way to proceed, as, at this point, the structure of obtained products is unknown. The correct approach is to consider the deviations of computed versus experimental values. For this strategy, the mean absolute errors (MAEs), and root-mean-square deviations (RMSDs) were calculated with the result that for all computational methods, structures **4** and **5** gave the best match with the experiment.

In the next step, the experimentally observed chemical shifts of other protons need to be included. In the case of structures **4**, the proton attached to the second nitrogen atom must give a broad peak, which is absent in the experimental spectrum of alkylated products. Structures **5a-g** do not contain a proton near the exocyclic nitrogen, whereas in all experimental spectra of the obtained products, the signals of these protons are found in the range of 6.50–8.36 ppm. Obviously, at this point, the predicted ^{1}H NMR spectra are not useful in resolving the structures of the alkylated products. Which is due to very close values of chemical shifts calculated for structures **3, 4, 5** (see Table 2). Nevertheless, a few trends can be noted. In the case of PBE functional, increasing the basis set size decreases the correlation in general. The MAE and RMSD values are higher for PBE/λ3 than for PBE/6–31G(d), whereas the values of R^2 are lower. Similar, but less pronounced differences are present in the case of B3LYP functional. In general, a slightly better correlation was obtained with the 6–31G(d) basis set.

In a similar manner the ^{13}C NMR chemical shifts were analyzed (see Table 3). The comparison of computed versus experimental chemical shift values show that for all chosen theoretical levels, MAE and RMSD values are lowest in the case of structures **3**. In addition, the absolute values of intercepts are also the smallest for this type of geometries. These computations clearly testify the formation of thioethers **3a-h** via the alkylation of the exocyclic sulfur atom. This result is in full agreement with previous studies, where alkylation of the exocyclic thione sulfur was proven by XRD technique [10,31,77].

In the case of PBE calculations, a great improvement when using of λ3 basis set instead of 6–31G(d) is noteworthy. For λ3, the MAE and RSMD values are only 2.4 and 2.3 ppm, respectively; whereas for 6–31G(d), the MAE equals 5.1 ppm and RMSD equals 4.6 ppm. However, the correlation coefficients R^2 are very similar for both the 6–31G(d) and the λ3 basis set. In the case of B3LYP functional, the quality of observed correlations slightly decreases when the polarization function is added to the hydrogen atoms. Applying the 6–31G(d) basis, the MAE and RMSD values equal 4.1 and 3.6 ppm, respectively; whereas, when using the 6–31G(d,p) basis set, the MAE and RMSD values increase to 4.8 and 4.2 ppm, respectively.

Knowing that the alkylation of model triazole-2-thione leads to the formation of structures **3**, we can improve the GIAO DFT-based method for the prediction of NMR chemical shifts of the hydrocarbon group attached to the sulfur atom in alkylsulfanyl-substituted 1,2,4-triazoles. The prediction capability increases when considering a linear correlation between DFT-computed and experimental chemical shifts:

δ(predicted) = δ(DFT)*S – I where δ(predicted) is the predicted value of NMR chemical shift, δ(DFT) is the chemical shift calculated with DFT methods, S and I are corresponding slopes and intercepts, respectively, from Tables 2 or 3. These calculations reduce the MAE and RMSD values, whereas the R^2 values remain the same (see Table 4). The B3LYP/6–31G(d) method is found to be the most preferable as it delivers good results even with relatively small basis set. Thus, in both ^{1}H and ^{13}C NMR calculations, this method results in MAE of 0.157 and 0.773 ppm, respectively, and RMSD values of 0.192 and 1.123 ppm, respectively.

Table 2
Correlation between experimental and GIAO computed ^{1}HNMR chemical shifts (in ppm) of the protons attached to the α-carbon of the alkyl group introduced to the triazole core. S – slope, I – intercept, R^2 – correlation coefficient, MAE –mean absolute error, RMSD – root-mean-square deviation.

		a	b	c	d	e	f	g	h	i	j	S	I	R^2	MAE	RMSD
	EXP	4.39	4.22	3.79	3.6	2.5	3.79	3.56	2.38	3.77	3.22	–	–	–	–	–
PBE/6–31G(d)	1	4.59	4.57	4.41	4.15	3.15	4.28	4.00	3.18	4.30	3.70	1.227	−1.425	0.970	0.511	0.535
	2	4.95	5.06	4.80	4.62	3.50	4.74	4.51	2.71	4.56	4.01	0.853	−0.185	0.912	0.824	0.851
	3	4.45	4.50	4.12	4.32	2.50	4.49	4.20	2.88	4.25	3.37	0.845	0.221	0.868	0.387	0.461
	4	3.90	4.23	3.56	3.46	2.64	3.60	3.68	2.87	–	–	1.330	1.116	0.892	0.226	0.278
	5	4.15	4.24	3.36	3.77	2.46	4.05	3.72	2.17	–	–	0.892	0.418	0.905	0.192	0.228
PBE/λ3	1	4.93	4.95	4.85	4.42	3.31	4.59	4.29	3.39	4.72	4.03	1.065	−1.108	0.951	0.826	0.838
	2	5.38	5.53	5.41	5.08	3.84	5.22	4.87	3.02	4.93	4.28	0.771	−0.143	0.896	1.235	1.264
	3	4.65	4.70	4.46	4.59	2.64	4.78	4.48	3.23	4.48	3.47	0.790	0.244	0.814	0.626	0.698
	4	4.30	4.61	3.99	3.81	2.85	3.98	4.08	3.05	–	–	1.168	−0.950	0.916	0.328	0.375
	5	4.50	4.51	3.66	3.93	2.56	4.32	3.93	2.25	–	–	0.822	0.480	0.935	0.244	0.288
B3LYP/6–31G(d)	1	4.92	5.96	4.61	4.39	3.46	4.51	4.31	3.47	4.58	4.01	0.810	0.057	0.792	0.900	0.953
	2	5.04	5.17	4.91	4.69	3.68	4.82	4.60	3.55	4.67	4.14	1.160	1.720	0.960	1.005	1.016
	3	4.42	4.49	4.07	4.24	2.59	4.42	4.16	2.53	4.18	3.30	0.831	0.331	0.905	0.319	0.391
	4	4.20	4.38	3.72	3.62	2.81	3.77	3.80	3.05	–	–	1.331	1.357	0.921	0.209	0.289
	5	4.21	4.40	3.44	3.90	2.65	4.19	3.84	2.25	–	–	0.882	0.345	0.883	0.245	0.262
B3LYP/6–31G(d,p)	1	4.96	4.87	4.74	4.44	3.50	4.02	4.34	3.53	4.67	4.09	1.169	−1.522	0.865	0.794	0.831
	2	5.12	5.25	5.11	4.82	3.79	4.95	4.67	3.36	4.76	4.20	1.015	−1.150	0.929	1.080	1.092
	3	4.44	4.50	4.16	4.33	2.64	4.52	4.25	3.17	4.25	3.29	0.892	−0.006	0.816	0.433	0.514
	4	4.22	4.48	3.87	3.71	2.87	3.86	3.91	3.08	–	–	1.300	−1.345	0.923	0.263	0.328
	5	4.25	4.44	3.53	3.92	2.67	4.21	3.85	2.26	–	–	0.882	0.315	0.899	0242	0.260

Table 3
Correlation between experimental and GIAO computed ^{13}C NMR chemical shifts (in ppm) of the protons attached to the α-carbon of the alkyl group introduced to the triazole core. S – slope, I – intercept, R^2 – correlation coefficient, MAE – mean absolute error, RMSD – root-mean-square deviation.

		a	b	c	d	e	f	g	h	i	j	S	I	R^2	MAE	RMSD
	EXP	37.0	37.2	21.7	35.7	14.9	36.0	40.6	15.5	34.8	33.5	–	–		–	–
PBE/6–31G(d)	1	54.0	55.3	42.5	54.7	36.0	54.4	56.2	33.2	53.7	50.4	1.096	−23.07	0.976	18.3	16.6
	2	53.1	52.6	38.3	52.2	34.2	52.4	54.4	34.0	52.1	50.4	1.139	−23.27	0.989	16.7	14.9
	3	43.6	43.5	27.9	40.7	18.7	41.7	42.8	18.9	41.6	38.4	0.940	−2.95	0.978	5.1	4.6
	4	60.0	50.3	41.8	54.0	37.8	54.2	55.2	37.0	–	–	1.249	−30.61	0.940	18.6	18.8
	5	53.7	55.5	45.6	55.1	36.0	59.0	57.9	32.9	–	–	1.010	−20.15	0.934	19.6	19.8
PBE/λ3	1	51.4	53.0	39.6	52.6	30.8	52.1	54.5	27.7	51.8	48.5	0.952	−13.30	0.971	15.5	13.8
	2	50.2	49.8	34.9	50.2	29.1	50.1	52.2	28.8	49.6	48.4	1.006	−13.90	0.988	13.6	12.0
	3	40.0	39.9	23.2	37.3	11.7	38.2	39.2	11.9	38.2	35.0	0.821	4.87	0.974	2.4	2.3
	4	55.2	48.4	39.1	52.7	33.9	52.6	54.1	32.3	–	–	1.091	−20.40	0.947	16.2	16.4
	5	51.2	53.4	42.7	53.3	30.8	57.9	56.3	28.0	–	–	0.879	−11.23	0.926	16.9	17.1
B3LYP/6–31G(d)	1	53.5	55.0	42.0	54.7	36.6	54.4	56.3	34.1	54.0	50.9	1.133	−25.01	0.979	18.5	16.6
	2	52.7	52.5	37.9	52.1	34.7	52.2	54.6	34.4	52.3	50.6	1.154	−23.98	0.986	16.7	14.9
	3	42.3	42.2	26.0	39.5	18.4	40.5	42.0	18.6	40.5	38.1	0.962	−2.82	0.985	4.1	3.6
	4	56.0	50.2	41.0	53.2	37.8	53.2	54.8	37.1	–	–	1.305	−32.69	0.950	18.1	18.4
	5	53.0	54.7	44.8	54.3	36.3	57.9	57.3	32.9	–	–	1.056	−21.8	0.939	19.1	19.2
B3LYP/6–31G(d,p)	1	54.1	55.6	42.6	55.3	36.8	56.0	57.0	34.3	54.6	51.4	1.101	−24.10	0.977	19.1	17.2
	2	53.2	53.0	38.5	52.6	34.8	52.8	55.2	34.5	52.7	51.0	1.138	−23.77	0.988	17.1	15.3
	3	43.1	43.1	26.9	40.4	18.7	41.3	42.8	18.8	41.3	38.8	0.943	−2.81	0.984	4.8	4.2
	4	56.6	50.9	41.6	53.8	38.1	53.8	55.5	37.3	–	–	1.282	−32.3	0.955	18.6	18.9
	5	53.7	55.3	45.5	54.9	36.4	58.5	58.0	33.0	–	–	1.033	−21.2	0.939	19.6	19.7

Table 4
Errors in accuracy of chosen GIAO DFT methods for prediction of NMR chemical shifts of R-$\underline{CH_2}$-S group in 1,2,4-triazoles.

Method	^{1}H NMR			^{13}C NMR		
	MAE	RMSD	R^2	MAE	RMSD	R^2
PBE/6–31G(d)	0.205	0.227	0.868	0.997	1.330	0.978
PBE/λ3	0.233	0.269	0.814	1.021	1.466	0.974
B3LYP/6–31G(d)	0.157	0.192	0.905	0.773	1.123	0.985
B3LYP/6–31G(d,p)	0.235	0.268	0.816	0.815	1.157	0.984

3.2. Reactivity of triazoles a-d

To explain the observed regioselective electrophilic attack of the exocyclic sulfur atom in 1,2,4-triazol-3-thiones, several reactivity descriptors were computed at the PBE0/6311++G(d,p) level of theory. Geometry optimization of forms of **a-d** was performed with the PBE/6–31G(d) method and optimized structures can be found in Supplementary materials (Tables S1–4). As the alkylation was performed in alkaline and in neutral mediums, the different forms of triazoles **a-d** must be considered. While the anionic states of **a-d** are the predominant forms in an alkaline solution, a mixture of thione (major) and thiol (minor) isomers are the major forms in a neutral solution. As the experiments were performed in ethanol, the CPCM with appropriate parameters was included in all computations. For clarity, the numbering in the triazole ring in this section is consistent with Scheme 1.

At first, the highest occupied molecular orbital (HOMO) must be considered as the isosurface determining the reactivity of the considered triazoles (see Fig. 1). In all cases, HOMO is located over the whole 1,2,4-triazole-3-thione system for all triazoles. The contribution of the pyrrole-type nitrogen in position 4 of the ring in the case of an attached phenyl group to the HOMO isosurface is negligible, which can be explained by the participation of the nitrogen atom's lone electron pair in the conjugation of the triazole aromatic system. However, an exocyclic nitrogen atom, if present, contributes to the HOMO isosurface. In addition, we have noticed a significant influence of the phenyl and phenylamino groups in

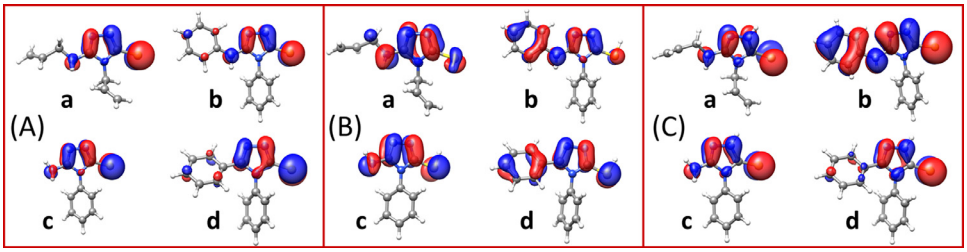

Fig. 1. HOMOs of anionic (A), thiol (B), and thione (C) forms of triazoles **a-d**.

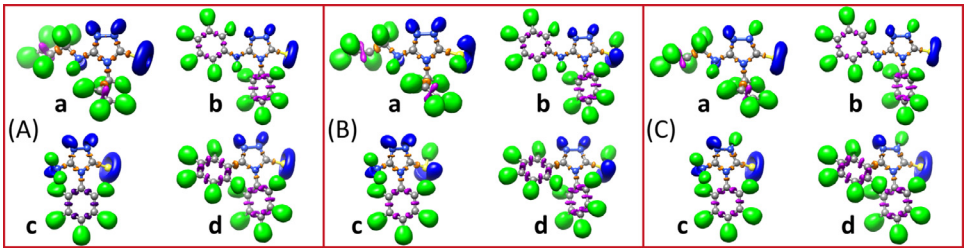

Fig. 2. ELFs of anionic (A), thiol (B), and thione (C) forms of triazoles **a-d**.

the HOMO formation of thiols **b** and **d**. While the contribution of the 5-phenyl group of thione **d** into the HOMO is minimal, the 5-phenylamino group of thione **b** has a high impact on the HOMO. In general, the analysis of the HOMO isosurfaces reveals that the 5-R(amino)-1,2,4-triazole-3-thione system, except for the pyrrole-type nitrogen atom, is the most reactive compound of the molecules **a-d**. However, these calculations do not allow for grading the influence of the different atoms on HOMO and for determining the most reactive atom.

Electron localization function (ELF) allows the mapping of the probability of the location of electron pairs. In Fig. 2, the ELFs of the anionic, thiol, and thione forms of triazoles **a-d** are shown. The large green domains correspond to hydrogen atoms, and the blue blobs represent lone pair domains. Relatively small yellow and purple areas correspond to covalent bond domains. Yellow and purple colors were used to grade the blobs area size. Larger purple areas are observed in phenyl rings and double bonds of allyl fragments, while single bonds and bonds in the triazole ring are characterized by much smaller yellow areas. A low ELF in the triazole ring indicates a lower delocalization of electrons over the ring and, consequently, its lower aromatic character in comparison to phenyl rings. The lone pair electrons can be donated to the unoccupied orbitals of electrophiles (alkylation agents). Considering the areas of lone pair domains, the reactivity of the heteroatoms can be graded as follows: (a) the sulfur atom is the most reactive center; (b) the nitrogen atoms in positions 1 and 2 of the triazole ring are slightly less reactive, while in the case of thione forms (Fig. 2C), the second nitrogen atom is not reactive at all; (c) the exocyclic nitrogen atom in triazoles **a-c** exhibits the lowest reactivity. In the case of thiols, a noticeable decrease of the ELF near the sulfur can be explained by the sharing of some electron density with the attached hydrogen atom.

The Fukui function for an electron elimination process (f^-), the so-called electrophilic Fukui function, determines the preferable site of the attack of an electrophile. This function was used to explain the regioselectivity of the alkylation of triazoles **a-d**. The high prediction capability of Fukui functions in electrophilic reactions, like protonation [78] and alkylation [79,80] has been reported. In Fig. 3, the electrophilic Fukui functions of the anionic, thiol, and thione forms of **a-d** are presented. Light blue areas represent positive and purple areas negative values. The highest values of the Fukui function determine the most favorable site for electrophilic attack. In the case of anionic and thione species, the largest isosurface areas are located on the sulfur atom, which concurs with the experimentally observed S-alkylation. The reactivity of the sulfur significantly decreases in thiols **c** and **d**, and becomes negligible in thiols **a** and **b**. Oppositely, the reactivity of the exocyclic nitrogen increases. However, these results do not contradict the experiment, as the thiol forms are less stable then thione, and consequently, thiols are present in reaction mixture only at a trace level. To support this statement, the total energies, total enthalpies, relative Gibbs free energies, and isomers distribution values of thione and thiol forms of **a-d** are presented in Table 5.

All data presented in Table 5 were calculated at the CPCM-PBE0/6–311++G(d,p)//PBE/6–31G(d) level of theory for the gas phase, ethanol and DMSO CPCM solutions. Comparing the relative Gibbs free energies at 25 °C, it can be observed that in all cases, the thione form is about 10.9–14.8 kcal/mol more stable than the corresponding thiol. Therefore, the major fraction of triazoles **a-d** exists in the thione form. Furthermore, increasing the electron donating ability of the substituent in position 5 of the triazole ring leads to the increase of the stability of thione form. The calculated distributions of respective thione/thiol forms indicate the presence of only traces of thiols in solution, which do not influence the regioselectivity of the alkylation reaction.

The reactive sites of electrophile-nucleophile interactions can be described through the analysis of atomic partial charges. The different types of atomic partial charges of exocyclic nitrogen (N5), nitrogen atoms in position 1 (N1) and 2 (N2) of the triazole ring, and exocyclic sulfur (S3) are presented in Table 6. To support the observed regioselectivity of alkylation at the sulfur atom, the calculated partial charges should be most negative at the S3 sulfur atom. All types of partial charges were calculated at the CPCM(Ethanol)-PBE0/6–311++G(d,p) level of theory, except the Mulliken and Löwdin charges; since these two population schemes are not consistent with basis sets containing diffuse functions, the CPCM(Ethanol)-PBE0/6–311G(d,p) method was used for the calculation of these types of partial charges.

According to Table 6, none of the studied types of partial charges predicts the sulfur as the preferred reaction center in thiol forms. However, it cannot be considered as a limitation of the approach since the thiols rearrange to their thione form and experimental evidences of regioselectivity of the thiol cannot be obtained. In the case of the anionic and thione forms, the Hirshfeld

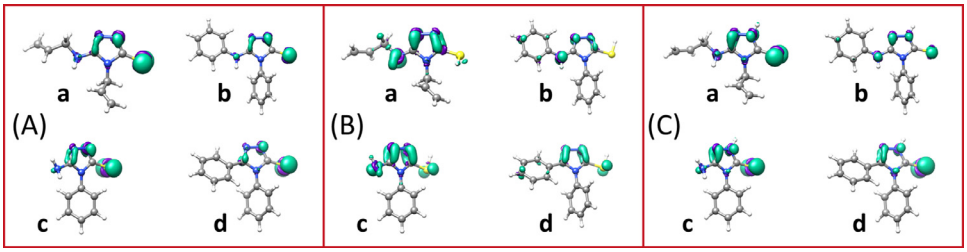

Fig. 3. Electrophilic Fukui functions of anionic (A), thiol (B), and thione (C) forms of triazoles **a-d**.

Table 5
Total energies (E, Ha), total enthalpies (H, Ha), relative Gibbs free energies at 25 °C (G, kcal/mol), and isomers distribution values (D,%) of thione and thiol forms of **a-d** in gas phase (Gas), ethanol (Ethanol) and DMSO (DMSO) solutions calculated at the PBE0/6–311++G(d,p)//PBE/6–31G(d) (PBE0) level of theory.

Level of theory		**a**		**b**		**c**		**d**	
		Thione	thiol	thione	thiol	thione	thiol	thione	thiol
Ethanol	E	−928.632	−928.606	−1157.111	−1157.088	−926.288	−926.264	−1101.799	−1101.777
	H	−928.420	−928.398	−1156.860	−1156.840	−926.120	−926.100	−1101.565	−1101.546
	G	0.00	13.29	0.00	11.81	0.00	12.51	0.00	10.88
	D	100.00	1.81×10^{-8}	100.00	2.22×10^{-7}	100.00	6.74×10^{-8}	100.00	1.06×10^{-6}
Gas	E	−928.609	−928.581	−1157.088	−1157.064	−926.264	−926.240	−1101.778	−1101.756
	H	−928.397	−928.373	−1156.836	−1156.816	−926.096	−926.075	−1101.544	−1101.526
	G	0.00	14.75	0.00	12.21	0.00	12.58	0.00	10.86
	D	100.00	1.55×10^{-9}	100.00	1.11×10^{-7}	100.00	5.95×10^{-8}	100.00	1.09×10^{-6}
DMSO	E	−928.632	−928.607	−1157.112	−1157.089	−926.289	−926.265	−1101.799	−1101.777
	H	−928.420	−928.398	−1156.861	−1156.841	−926.121	−926.100	−1101.565	−1101.547
	G	0.00	13.23	0.00	11.78	0.00	12.50	0.00	10.87
	D	100.00	2.02×10^{-8}	100.00	2.30×10^{-7}	100.00	6.81×10^{-8}	100.00	1.07×10^{-6}

Table 6
DFT-computed partial atomic charges of N1, N2, S3, and N5 atoms in anionic, thione, and thiol forms of triazoles **a-d**. The match of calculated partial charges with observed regioselectivity highlighted boldly.

Charges	Atom	anion				thione				thiol			
		a	**b**	**c**	**d**	**a**	**b**	**c**	**d**	**a**	**b**	**c**	**d**
ADCH	N1	−0.513	−0.432	−0.443	−0.359	−0.397	−0.285	−0.211	−0.413	−0.445	−0.550	−0.539	−1.034
	N2	−0.409	−0.670	−0.759	−0.564	−0.079	−0.431	−0.616	−0.052	−0.176	−0.151	−0.189	0.186
	S3	**−0.693**	**−0.885**	**−0.924**	**−0.691**	**−0.475**	**−0.513**	**−0.521**	**−0.471**	−0.124	−0.057	−0.038	−0.014
	N5	−0.432	−0.396	−0.657	–	−0.376	−0.379	−0.635	–	−0.364	−0.450	−0.633	–
CM5	N1	−0.378	−0.419	−0.392	−0.334	−0.317	−0.296	−0.324	−0.275	−0.344	−0.324	−0.359	−0.310
	N2	−0.410	−0.476	−0.401	−0.380	−0.296	−0.292	−0.294	−0.279	−0.334	−0.341	−0.344	−0.330
	S3	**−0.626**	**−0.733**	**−0.614**	**−0.594**	−0.437	**−0.427**	−0.429	**−0.419**	−0.115	−0.099	−0.101	−0.094
	N5	−0.485	−0.518	−0.613	–	−0.465	−0.421	−0.592	–	−0.471	−0.425	−0.601	–
Hirshfeld	N1	−0.283	−0.251	−0.298	−0.239	−0.210	−0.186	−0.220	−0.166	−0.249	−0.351	−0.265	−0.213
	N2	−0.322	−0.308	−0.312	−0.295	−0.029	−0.024	−0.026	−0.013	−0.240	−0.523	−0.247	−0.234
	S3	**−0.617**	**−0.603**	**−0.606**	**−0.586**	**−0.425**	**−0.416**	**−0.418**	**−0.409**	−0.046	−0.226	−0.032	−0.025
	N5	−0.157	−0.101	−0.194	–	−0.129	−0.090	−0.164	–	−0.137	−0.917	−0.176	–
CHELPG	N1	−0.543	−0.306	−0.523	−0.421	−0.631	−0.495	−0.589	−0.529	−0.496	−0.225	−0.524	−0.451
	N2	−0.617	−0.690	−0.558	−0.597	0.106	−0.016	0.124	0.191	−0.523	−0.243	−0.405	−0.430
	S3	−0.827	−0.798	−0.803	−0.792	−0.498	−0.482	−0.475	−0.469	−0.263	−0.030	−0.211	−0.228
	N5	−0.880	−0.894	−0.890	–	−0.736	−0.813	−0.865	–	−0.823	−0.094	−0.879	–
NPA	N1	−0.449	−0.442	−0.454	−0.359	−0.386	−0.382	−0.385	−0.298	−0.428	−0.425	−0.427	−0.346
	N2	−0.482	−0.464	−0.471	−0.450	−0.398	−0.392	−0.395	−0.383	−0.369	−0.397	−0.404	−0.392
	S3	−0.542	−0.512	−0.520	−0.488	−0.338	−0.312	−0.317	−0.301	0.012	0.040	0.036	0.048
	N5	−0.677	−0.617	−0.849	–	−0.654	−0.607	−0.824	–	−0.665	−0.611	−0.836	–
Mulliken	N1	−0.386	−0.396	−0.383	−0.328	−0.315	−0.329	−0.308	−0.257	−0.371	−0.388	−0.364	−0.323
	N2	−0.379	−0.358	−0.368	−0.345	−0.287	−0.276	−0.282	−0.265	−0.291	−0.305	−0.318	−0.300
	S3	**−0.619**	**−0.585**	**−0.600**	**−0.567**	−0.376	−0.347	−0.358	−0.339	−0.004	0.022	0.014	0.028
	N5	−0.509	−0.561	−0.538	–	−0.506	−0.565	−0.523	–	−0.513	−0.568	−0.532	–
Löwdin	N1	−0.175	−0.157	−0.179	−0.115	−0.110	−0.098	−0.111	−0.045	−0.153	−0.139	−0.155	−0.095
	N2	−0.205	−0.191	−0.196	−0.187	0.152	0.157	0.154	0.163	−0.111	−0.129	−0.135	−0.128
	S3	**−0.480**	**−0.456**	**−0.465**	**−0.433**	**−0.257**	**−0.237**	**−0.243**	**−0.227**	0.243	0.263	0.257	0.270
	N5	0.015	0.104	0.011	–	0.050	0.117	0.054	–	0.037	0.111	0.036	–

population scheme and its successor ADCH produce partial charges that are in agreement with the observed reaction path. This result is expected, as a good prediction capability of Hirshfeld partial charges was reported previously [81–84]. The CM5 partial charges are very similar. In the case of thiones **a** and **c**, the N5 atom indicated as more negative and therefore as the preferred reaction center, which is not in accordance with the experimental results.

The CHELPG and NPA partial charges were found inadequate for this type of analysis. This finding is surprising, considering that the CHELPG scheme was created to reproduce electrostatic potential in the most optimal way and that these charges were expected to be suitable for the description of strong polar interactions. The failure of the NPA scheme is also not explainable, especially considering its good performance in the prediction of physico-chemical proper-

ties, like LogP [85]. Mulliken population analysis results in correct predictions in the case of anionic forms, but fails for the model thione species. The Löwdin partial charges are found very suitable for the prediction of S-alkylation of anionic and thione forms, and thus, could be used for the modeling of analogues systems.

Conclusions

Ten S-alkylated triazoles were synthesized through the alkylation of four 1,2,4-triazole-3-thiones with eight different alkyl halides; seven of the obtained 3-alkylsulfanyl-1,2,4-triazoles are new and have not been previously described in the literature.

The sole comparison of ^{1}H NMR spectra with GIAO DFT-computed chemical shifts is not a reliable approach to reveal the structure of alkylation products. The presence of several reactive centers in the different possible structural forms of the considered triazoles determines the subsequent formation of the different alkylation products, which are characterized by relatively close isotropic chemical shielding values of characteristic groups. The analysis of experimentally observed and GIAO calculated ^{13}C NMR chemical shifts of the α-methylene(methyl) group of the introduced hydrocarbon fragment allows for the reliable assignment of the experimental peaks to S-alkyl groups. A strong correlation (MAE = 0.773 ppm, RMSD = 1.123 ppm, R^2 = 0.985) was obtained between experimental and calculated values of ^{13}C NMR chemical shifts of the characteristic carbon.

The anionic, thione and thiol forms of the triazoles **a-d** were studied in terms of DFT reactivity descriptors to provide insight into the observed alkylation regioselectivity. The anionic form of the used 1,2,4-triazoles is predominant in alkaline medium, whereas the thione and thiol forms were considered as the major species in a neutral solution. However, due to the very low quantity of thiols, the impact of these forms can be considered as negligible. Thus, PBE0/6–311++G(d,p) computations reveal that thiones are about 10.9–13.3 kcal/mol more stable than the corresponding thiols, and that the thione stability increases with the increasing the electron donating ability of the substituent in position 5 of the triazole ring.

ELF and Fukui function isosurfaces can correctly predict the observed preferential reactivity of the exocyclic sulfur atom in the anionic and thione forms. Oppositely, HOMOs are found not to be suitable for this prediction. Among several tested types of atomic partial charges, only Hirshfeld, ADCH, and Löwdin population schemes can correctly predict the preferential attack on the S-atom.

Author credit statements

Maksym Fizer: Conceptualization, Supervision, Investigation, Writing - Original Draft, Writing - Review & Editing. **Mikhailo Slivka**: Conceptualization, Investigation, Writing - Original Draft, Writing - Review & Editing. **Nataliya Korol:** Investigation, Writing - Original Draft. **Oksana Fizer**: Investigation, Writing - Original Draft, Writing - Review & Editing.

Declaration of Competing Interest

The authors declare that they have no known competing financial interests or personal relationships that could have appeared to influence the work reported in this paper.

Acknowledgments

This work was partially financially supported by the Ministry of Education and Science of Ukraine (Projects GR-0119U100232 and GR-0120U100431).

References

[1] V. Shah, Ch. Yang, Z. Shen, B.M. Kerr, K. Tieu, D.M. Wilson, J. Hall, M. Gillen, C.A. Lee, Metabolism and disposition of lesinurad, a uric acid reabsorption inhibitor, in humans, Xenobiotica 49 (2019) 811–822 https://doi.org/10.1080/00498254.2018.1504257.

[2] M.M. Regeda-Furdychko, The influence of thiotriazoline on the indicators of nitric oxide under the condition of experimental contact dermatitis and experimental pneumonia, J. Edu. Health Sport 10 (2020) 35–40 http://doi.org/10.12775/JEHS.2020.10.02.004.

[3] M.C.F.C.B. Damião, R. Galaverna, A.P. Kozikowski, J. Eubanks, J.C. Pastre, Telescoped continuous flow generation of a library of highly substituted 3-thio-1,2,4-triazoles, React. Chem. Eng. 2 (2017) 896–907 https://doi.org/10.1039/C7RE00125H.

[4] A.T.A. Boraei, A new direct synthetic access to 4-amino-2-N-(glycosyl/propyl)-1,2,4-triazole-3-thiones via hydrazinolysis of 3-N-((acylatedglycosyl)/allyl)-1,3,4-oxadiazole-2-thiones, Arkivoc 3 (2016) 71–81 https://doi.org/10.3998/ark.5550190.p009.399.

[5] A.T.A. Boraei, E.S.H. El Ashry, A. Duerkop, Regioselectivity of the alkylation of S-substituted 1,2,4-triazoles with dihaloalkanes, Chem. Cent. J. 10 (2016) 22–35 https://doi.org/10.1186/s13065-016-0165-0.

[6] A.T.A. Boraei, M.S. Gomaa, E.S.H.E. Ashry, A. Duerkop, Design, selective alkylation and X-ray crystal structure determination of dihydro-indolyl-1,2,4-triazole-3-thione and Its 3-benzylsulfanyl analogue as potent anticancer agents, Eur. J. Med. Chem. 125 (2017) 360–371 https://doi.org/10.1016/j.ejmech.2016.09.046.

[7] M.V. Slivka, N.I. Korol, V. Pantyo, V.M. Baumer, V.G. Lendel, Regio- and stereoselective synthesis of [1,3]thiazolo[3,2-*b*][1,2,4]triazol-7-ium salts via electrophilic heterocyclization of 3-Spropargylthio-4H-1,2,4-triazoles and their antimicrobial activity, Heterocycl. Commun. 23 (2017) 109–114 https://doi.org/10.1515/hc-2016-0233.

[8] N. Korol, M. Slivka, M. Fizer, V. Baumer, V. Lendel, Halo-heterocyclization of butenyl(prenyl)thioethers of 4,5-diphenyl-1,2,4-triazol-3-thiole into triazolo[5,1-]thiazinium systems: experimental and theoretical evolution, Monatsh. Chem. 151 (2020) 191–198 https://doi.org/10.1007/s00706-019-02545-w.

[9] M.A. Kaldrikyan, N.S. Minasyan, R.G. Melik-Ogandzhanyan, Synthesis of new 4,5-substituted 4*H*-1,2,4-triazole-3-thiols and their sulfanyl derivatives, Russ. J. Gen. Chem. 85 (2015) 622–627 https://doi.org/10.1134/S1070363215030160.

[10] T.R. Hovsepyan, F.G. Arsenyan, L.E. Nersesyan, A.S. Agaronyan, I.S. Danielyan, R.V. Paronikyan, R.G. Melik-Ogandzhanyan, Synthesis, transformations, and study of some biological properties of new 3,4,5-substituted 1,2,4-triazoles, Pharm. Chem. J. 49 (2015) 231–236 https://doi.org/10.1007/s11094-015-1261-5.

[11] M. Kalhor, M. Shabani, I. Nikokar, S.R. Banisaeed, Synthesis, characterization and antibacterial activity of some novel thiosemicarbazides, 1,2,4-triazol-3-thiols and their S-substituted derivatives, Iran. J. Pharm. Res. 14 (2015) 67–75.

[12] M.A. Samvelyan, T.V. Ghochikyan, S.V. Grigoryan, R.A. Tamazyan, A.G. Aivazyan, Alkylation of 1,2,4-triazole-3-thiols withhaloalkanoic acid esters, Russ. J. Org. Chem. 53 (2017) 935–940 https://doi.org/10.1134/S1070428017060203.

[13] L. Perekhoda, I. Kadamov, N. Saidov, V. Georgiyants, Synthesis of novel substituted 4-phenyl-5-phenoxymethyl-3-mercapto-1,2,4-triazole (4 H) derivatives as potential anti-ulcer agents, Scripta Scientica Pharmaceutica 2 (2015) 46–52.

[14] A.R. Faizullina, D.S. Blokhin, A.M. Kusova, V.V. Klochkov, Investigation of the effect of transition metals (MN, CO, GD) on the spatial structure of fibrinopeptide B by NMR spectroscopy, J. Mol. Struct. 1204 (2020) 127484 https://doi.org/10.1016/j.molstruc.2019.127484.

[15] G. Szalontai, ^{1}H NMR linewidths of small organic guest molecules physisorbed on different mesoporoussilicas, J. Mol. Struct. 1205 (2020) 127646 https://doi.org/10.1016/j.molstruc.2019.127646.

[16] P.C.S. Costa, M.R.O. Barsottini, M.L.L. Vieira, B.A. Pires, J.S. Evangelista, A.C.M. Zeri, A.F.Z. Nascimento, J.S. Silva, M.F. Carazzolle, G.A.G. Pereira, M.L. Sforça, P.C.M.L. Miranda, S.A. Rocco, N-Phenylbenzamide derivatives as alternative oxidase inhibitors: synthesis, molecular properties, ^{1}H-STD NMR, and QSAR, J. Mol. Struct. 1208 (2020) 127903 https://doi.org/10.1016/j.molstruc.2020.127903.

[17] M. Stolarska, W. Bocian, J. Sitkowski, B. Naumczuk, E. Bednarek, M. Popławska, A. Błażewicz, L. Kozerski, Cathinones - Routine NMR methodology for enantiomer discrimination and their absolute stereochemistry assignment, using R-BINOL, J. Mol. Struct. (2020) 128575 https://doi.org/10.1016/j.molstruc.2020.128575.

[18] I. Philipova, G. Stavrakov, V. Dimitrov, N. Vassilev, Galantamine derivatives: synthesis, NMR study, DFT calculations and application in asymmetric catalysis, J. Mol. Struct. 1219 (2020) 128568 https://doi.org/10.1016/j.molstruc.2020.128568.

[19] P.W. Szafrański, M.E. Trybuła, P. Kasza, M.T. Cegła, Following the oxidation state of organosulfur compounds with NMR: experimental data versus DFT calculations and database-powered NMR prediction, J. Mol. Struct. 1202 (2020) 127346 https://doi.org/10.1016/j.molstruc.2019.127346.

[20] A. Karayel, S. Özbey, C. Kuş, G. Ayhan-Kılcıgil, Restricted rotation around the methylene bridge of 5-(2-p-(chlorophenyl)benzimidazole-1- yl)methyl-4-(o-substitutedphenyl)-2,4-dihydro-[1,2,4]-triazole-3-thiones as evidenced by NMR, X-RAY and DFT studies and the importance of low energy rotational conformers, J. Mol. Struct. 1177 (2019) 476–484 https://doi.org/10.1016/j.molstruc.2018.09.083.

[21] U.D. Phalgune, K. Vanka, P.R. Rajamohanan, GIAO/DFT studies on 1,2,4-triazole-5-thiones and their propargyl derivatives, Magn. Reson. Chem. 51 (2013) 767–774 https://doi.org/10.1002/mrc.4012.
[22] F.V. Toukach, V.P. Ananikov, Recent advances in computational predictions of NMR parameters for the structure elucidation of carbohydrates: methods and limitations, Chem. Soc. Rev. 42 (2013) 8376–8415 https://doi.org/10.1039/C3CS60073D.
[23] K. Wolinski, J.F. Hilton, P. Pulay, Efficient implementation of the gauge independent atomic orbital method for NMR chemical shift calculations, J. Am. Chem. Soc. 112 (1990) 8251–8260 https://doi.org/10.1021/ja00179a005.
[24] D. Xin, C.A. Sader, U. Fischer, K. Wagner, P.-J. Jones, M. Xing, K.R. Fandrick, N.C. Gonnella, Systematic investigation of DFT-GIAO 15N NMR chemical shift prediction using B3LYP/cc-pVDZ: application to studies of regioisomers, tautomers, protonation states and N-oxides, Org. Biomol. Chem. 15 (2017) 928–936 https://doi.org/10.1039/C6OB02450E.
[25] F.L.P. Costa, P.F. Gomes, A.K. Silva, L.M. Lião, Conformational analysis, experimental and GIAO-DFT ^{13}C NMR chemical shift calculation on 2'-hydroxy-3,4,5-trimethoxy-chalcone, J. Braz. Chem. Soc. 28 (2017) 2130–2135 https://doi.org/10.21577/0103-5053.20170060.
[26] R. Mejía-Urueta, K. Mestre-Quintero, R. Vivas-Reyes, DFT-GIAO calculation of propertiesof 19F NMR and stability study of environmentally relevant perfluoroalkylsulfonamides (PFASAmide), J. Braz. Chem. Soc. 22 (2011) 2268–2274 1174 https://doi.org/10.1590/S0103-50532011001200005 .
[27] S.M. Khripak, M.V. Slivka, R.V. Vilkov, R.N. Usenko, V.G. Lendel, Regioselectivity of the monohalogenation of 4-allyl-3-allylamino-1,2,4-triazole-5-thione, Chem. Heterocycl. Compd. (N Y) 43 (2007) 781–785 https://doi.org/10.1007/s10593-007-0126-6.
[28] H.-Y. Wang, P.-S. Zhao, R.-Q. Li, S.-M. Zhou, Synthesis, crystal structure and quantum chemical study on 3-phenylamino-4-phenyl-1,2,4-triazole-5-thione, Molecules 14 (2009) 608–620 https://doi.org/10.3390/molecules14020608.
[29] M. Dobosz, M. Wujec, The reactions of hydroiodide of 2-amino-1-substitutedguanidine derivatives with aromatic isothiocyanates, Heterocycles 57 (2002) 1135–1141 https://doi.org/10.3987/COM-02-9461.
[30] E. Hoggarth, 251. Compounds related to thiosemicarbazide. Part II. 1-Benzoylthiosemicarbazides, J. Chem. Soc. (1949) 1163–1167 https://doi.org/10.1039/JR9490001163.
[31] M. Fizer, M. Slivka, R. Mariychuk, V. Baumer, V. Lendel, 3-Methylthio-4-phenyl-5-phenylamino-1,2,4-triazole hexabromotellurate: x-ray and computational study, J. Mol. Struct. 1161 (2018) 226–236 https://doi.org/10.1016/j.molstruc.2018.02.054.
[32] M.D. Hanwell, D.E. Curtis, D.C. Lonie, T. Vandermeersch, E. Zurek, G.R. Hutchison, Avogadro: an advanced semantic chemical editor, visualization, and analysis platform, J. Cheminform 4 (2012) 17 https://doi.org/10.1186/1758-2946-4-17.
[33] T.A. Halgren, Merck molecular force field. I. Basis, form, scope, parameterization, and performance of MMFF94, J. Comput. Chem. 17 (1996) 490–519 https://doi.org/10.1002/(SICI)1096-987X(199604)17:5/6⟨490::AID-JCC1⟩3.0.CO;2-P.
[34] J.P. Perdew, K. Burke, M. Ernzerhof, Generalized gradient approximation madesimple, Phys. Rev. Lett. 77 (1996) 3865–3868 https://doi.org/10.1103/PhysRevLett.77.3865.
[35] M. Ernzerhof, G.E. Scuseria, Assessment of the perdew-burke-ernzerhofexchange-correlation functional, J. Chem. Phys. 110 (1999) 5029–5036 https://doi.org/10.1063/1.478401.
[36] D.N. Laikov, A. Ustynyuk Yu, PRIRODA-04: a quantum-chemical programsuite. New possibilities in the study of molecular systems with the applicationof parallel computing, Russ. Chem. Bull. Int Ed. 54 (2005) 820–826 https://doi.org/10.1007/s11172-005-0329-x.
[37] D. Laikov, Atomic basis functions for molecular electronic structure calculations, Theor. Chem. Acc. 138 (2019) 40 https://doi.org/10.1007/s00214-019-2432-3.
[38] A.D. Becke, A new mixing of Hartree-Fock and local density-functional theories, J. Chem. Phys. 98 (1993) 1372–1377 https://doi.org/10.1063/1.464304.
[39] F. Neese, Software update: the ORCA program system, version 4.0, WIREs Comput, Mol. Sci. 8 (2018) e1327 https://doi.org/10.1002/wcms.1327.
[40] V. Barone, M. Cossi, Quantum calculation of molecular energies and energy gradientsin solution by a conductor solvent model, J. Phys. Chem. A 102 (1998) 1995–2001 https://doi.org/10.1021/jp9716997.
[41] C. Adamo, V. Barone, Toward reliable density functionalmethodswithout adjustableparameters: the PBE0 model, J. Chem. Phys. 110 (1999) 6158–6170 https://doi.org/10.1063/1.478522.
[42] M.G. Medvedev, I.S. Bushmarinov, J. Sun, J.P. Perdew, K.A. Lyssenko, Density functionaltheory is straying from the path toward the exact functional, Science 355 (2017) 5975 https://doi.org/10.1126/science.aah5975.
[43] P. Fuentealba, R. Contreras, Fukui function in chemistry, Rev. Modern Quantum Chem. (2002) 1013–1052 https://doi.org/10.1142/9789812775702_0034.
[44] P. Fuentealba, E. Chamorro, J.C. Santos, Chapter 5 Understanding and using the electron localization function, Theoret. Comput. Chem. 19 (2007) 57–85 https://doi.org/10.1016/S1380-7323(07)80006-9.
[45] T. Lu, F. Chen, Multiwfn: a multifunctional wavefunction analyzer, J. Comput. Chem. 33 (2012) 580–592 https://doi.org/10.1002/jcc.22885.
[46] R.S. Mulliken, Electronic population analysis on LCAO-MO molecular wave functions, J. Chem. Phys. 23 (1955) 1833–1840 https://doi.org/10.1063/1.1740588.
[47] P.-O. Löwdin, On the nonorthogonality problem, Adv. Quant. Chem. 5 (1970) 185–199 https://doi.org/10.1016/S0065-3276(08)60339-1.
[48] C.M. Breneman, K.B. Wiberg, Determining atom-centered monopoles from molecular electrostatic potentials. The need for high sampling density in formamide conformational analysis, J. Comput. Chem. 11 (1990) 361–373 https://doi.org/10.1002/jcc.540110311.
[49] F.L. Hirshfeld, Bonded-atom fragments for describing molecular charge densities, Theor. Chim. Acta 44 (1977) 129–138 https://doi.org/10.1007/BF00549096.
[50] A.V. Marenich, S.V. Jerome, C.J. Cramer, D.G. Truhlar, Charge model 5, Charge model 5: an extension of Hirshfeld population analysis for the accurate description of molecular interactions in gaseous and condensed phases, J. Chem. Theory Comput. 8 (2012) 527–541 https://doi.org/10.1021/ct200866d.
[51] T. Lu, F. Chen, Atomic dipole moment corrected Hirshfeld population method, J. Theor. Comput. Chem. 11 (2012) 163–183 https://doi.org/10.1142/S0219633612500113.
[52] CM5charges, Version 1.0, H. Kruse.https://doi.org/10.5281/zenodo.1193754.
[53] A.E. Reed, R.B. Weinstock, F. Weinhold, Natural population analysis, J. Chem. Phys. 83 (1985) 735–746 https://doi.org/10.1063/1.449486.
[54] T.Y. Nikolaienko, L.A. Bulavin, D.M. Hovorun, JANPA: an open source crossplatformimplementation of the natural population analysis on the Java platform, Comput. Theor. Chem. 1050 (2014) 15–22 https://doi.org/10.1016/j.comptc.2014.10.002.
[55] E.F. Pettersen, T.D. Goddard, C.C. Huang, G.S. Couch, D.M. Greenblatt, E.C. Meng, T.E. Ferrin, UCSF Chimera – A visualization system for exploratory research and analysis, J. Comput. Chem. 25 (2004) 1605–1612 https://doi.org/10.1002/jcc.20084.
[56] D.N. Laikov, Fast evaluation of density functional exchange-correlation terms using the expansion of the electron density in auxiliary basis sets, Chem. Phys. Lett. 281 (1997) 151–156 https://doi.org/10.1016/S0009-2614(97)01206-2.
[57] F. Neese, An improvement of the resolution of the identity approximation for theformation of the Coulomb matrix, J. Comput. Chem. 24 (2003) 1740–1747 https://doi.org/10.1002/jcc.10318.
[58] F. Neese, F. Wennmohs, A. Hansen, U. Becker, Efficient, approximate and parallel Hartree-Fock and hybrid DFT calculations. A "chain-of-spheres" algorithm for theHartree-Fock exchange, Chem. Phys. 356 (2009) 98–109 https://doi.org/10.1016/j.chemphys.2008.10.036.
[59] E.S.H. El Ashry, L.F. Awad, S.M. Soliman, M.N.A. Al Moaty, H.A. Ghabbour, A. Barakat, Tautomerism aspect of thione-thiol combined with spectral investigation of some 4-amino-5-methyl-1,2,4-triazole-3-thione Schiff's bases, J. Mol. Struct. 1146 (2017) 432–440 https://doi.org/10.1016/j.molstruc.2017.06.002.
[60] N. Özdemir, D. Türkpençe, Theoretical investigation of thione-thiol tautomerism, intermolecular double proton transfer reaction and hydrogen bonding interactions in 4-ethyl-5-(2-hydroxyphenyl)-2H-1,2,4-triazole-3(4H)-thione, Comput. Theor. Chem. 1025 (2013) 35–45 http://dx.doi.org/10.1016/j.comptc.2013.10.001.
[61] T. Mroczek, T. Plech, M. Wujec, Novel concept of discrimination of1,2,4-triazole-3-thione and 3-thiol tautomers, J. Chromatogr. Sci. 55 (2017) 117–129 http://dx.doi.org/10.1093/chromsci/bmw151.
[62] M.D. Davari, H. Bahrami, Z.Z. Haghighi, M. Zahedi, Quantum chemical investigation of intramolecular thione-thiol tautomerism of 1,2,4-triazole-3-thione and its disubstituted derivatives, J. Mol. Model. 16 (2010) 841–855 http://dx.doi.org/10.1007/s00894-009-0585-z.
[63] O. Fedyshyn, Y. Bazeľ, M. Fizer, V. Sidey, J. Imrich, M. Vilkova, O. Barabash, Y. Ostapiuk, O. Tymoshuk, Spectroscopic and computational study of a new thiazolylazonaphthol dye 1-[(5-(3-nitrobenzyl)-1,3-thiazol-2-yl)diazenyl]naphthalen-2-ol, J. Mol. Liq. 304 (2020) 112713 https://doi.org/10.1016/j.molliq.2020.112713.
[64] M. Fizer, O. Fizer, V. Sidey, R. Mariychuk, Y. Studenyak, Experimental and theoreticalstudy on cetylpyridiniumdipicrylamide – a promising ion-exchanger forcetylpyridinium selective electrodes, J. Mol. Struct. 1187 (2019) 77–85 https://doi.org/10.1016/j.molstruc.2019.03.067.
[65] Y. Bazel, M. Leskova, M. Reclo, J. Sandrejova, A. Simon, M. Fizer, V. Sidey, Structuraland spectrophotometric characterization of 2-[4-(dimethylamino)styryl]-1-ethylquinolinium iodide as a reagent for sequential injection determination of tungsten, Spectrochim. Acta. Part A Mol. Biomol. Spectrosc. 196 (2018) 398–405 https://doi.org/10.1016/j.saa.2018.02.049.
[66] G.I. Csonka, A.D. French, G.P. Johnson, C.A. Stortz, Evaluation of density functionals and basis sets forcarbohydrates, J. Chem. Theory Comput. 5 (2009) 679–692 https://doi.org/10.1021/ct8004479.
[67] W.M.C. Sameera, D.A. Pantazis, A hierarchy of methods for the energetically accurate modeling of isomerism in monosaccharides, J. Chem. Theory Comput. 8 (2012) 2630–2645 https://doi.org/10.1021/ct3002305.
[68] M.W. Lodewyk, M.R. Siebert, D.J. Tantillo, Computational prediction of 1H and 13C chemical shifts: a useful tool for natural product, mechanistic, and synthetic organic chemistry, Chem. Rev. 112 (2012) 1839–1862 https://doi.org/10.1021/cr200106v.
[69] Y. Xia, H. Zhang, 13C NMR chemical shift prediction of diverse chemical compounds, SAR QSAR Environ. Res. 30 (2019) 477–490 https://doi.org/10.1080/1062936X.2019.1619621.
[70] F.L.P. Costa, A.C.F. de Albuquerque, F.M. dos Santos Junior, M.B. de Amorim, High cost-effectiveness ratio: GIAO-mPW1PW91/6-31G(d)//PM7 scaling factor for 13C NMR chemical shifts calculation, J. Comput. Theor. Nanosci. 12 (2015) 2195–2201 https://doi.org/10.1166/jctn.2015.4007.
[71] A.M. Sarotti, Successful combination of computationally inexpensive GIAO 13C NMR calculations and artificial neural network pattern recognition: a new strategy for simple and rapid detection of structural misassignments, Org. Biomol. Chem. 11 (2013) 4847–4859 https://doi.org/10.1039/c3ob40843d.

[72] E.Yu. Pankratyev, A.R. Tulyabaev, L.M. Khalilov, How reliable are GIAO calculations of ^{1}H and ^{13}C NMR chemical shifts? A statistical analysis and empirical corrections at DFT (PBE/3z) level, J. Comput. Chem. 32 (2011) 1993–1997 https://doi.org/10.1002/jcc.21786.
[73] P.A. Belaykov, V.P. Ananikov, Modeling of NMR spectra and signal assignment using real-time DFT/GIAO calculations, Russ. Chem. Bull., Int.Ed. 60 (2011) 783–789 http://dx.doi.org/10.1007/s11172-011-0405-3.
[74] M.A. Iron, Evaluation of the factors impacting the accuracy of 13C NMR chemical shift predictions using density functional theory – the advantage of long-range corrected functionals„ J. Chem. Theory Comput. 13 (2017) 5798–5819 http://dx.doi.org/10.1021/acs.jctc.7b00772.
[75] J.S. Lomas, 1H NMR spectra of alcohols in hydrogen bonding solvents: DFT/GIAO calculations of chemical shifts, Magn. Reson. Chem. 54 (2016) 28–38 https://doi.org/10.1002/mrc.4312.
[76] R. Jain, T. Bally, P.R. Rablen, Calculating accurate proton chemical shifts oforganic molecules with density functional methods and modest basis sets, J. Org. Chem. 74 (2009) 4017–4023.
[77] Ł. Popiołek, U. Kosikowska, L. Mazur, M. Dobosz, A. Malm, Synthesis and antimicrobial evaluation of some novel 1,2,4-triazole and 1,3,4-thiadiazole derivatives, Med. Chem. Res. 22 (2013) 3134–3147 https://doi.org/10.1007/s00044-012-0302-9.
[78] K. Bevziuk, A. Chebotarev, M. Fizer, A. Klochkova, K. Pliuta, D. Snigur, Protonation of Patented Blue V in aqueous solutions: theoretical and experimental studies, J. Chem. Sci. 130 (2018) 12 https://doi.org/10.1007/s12039-017-1411-2.
[79] S.B. Salah, R. Zaier, S. Ayachi, R. Goumont, T. Boubaker, The N-alkylation of 4-nitrobenzochalcogenadiazoles: synthesis and theoretical approach, J. Mol. Struct. 1197 (2019) 80–86 https://doi.org/10.1016/j.molstruc.2019.06.091.
[80] K.R. Santhy, M.D. Sweetlin, S. Muthu, C.S. Abraham, M. Raja, Molecular structure, spectroscopic (FT-IR, FT-Raman) studies, Homo-Lumo and Fukui function calculations of 2-Acetyl amino-5-bromo- 4 methyl pyridine by density functional theory, Chem. Data Collect. 24 (2019) 100291 https://doi.org/10.1016/j.cdc.2019.100291.
[81] B. Wang, Ch. Rong, P.K. Chattaraj, Sh. Liu, A comparative study to predict regioselectivity, electrophilicity and nucleophilicity with Fukui function and Hirshfeld charge, Theor. Chem. Acc. 138(2019) 124, https://doi.org/10.1007/s00214-019-2515-1.
[82] P. Bandyopadhyay, S. Raya, Md.M. Seikh, Unraveling the regioselectivity of odd electron halogen bond formation using electrophilicity index and chemical hardness parameters, Phys. Chem. Chem. Phys. 21 (2019) 26580–26590 https://doi.org/10.1039/C9CP05374C.
[83] M. Kut, M. Fizer, M. Onysko, V. Lendel, Reactions of N-alkenylthioureas with p-alkoxyphenyltelluriumtrichlorides, J. Heterocyclic Chem. 55 (2018) 2284–2290 https://doi.org/10.1002/jhet.3281.
[84] Sh. Liu, Quantifying reactivity for electrophilic aromatic substitution reactions with Hirshfeld charge, J. Phys. Chem. A 119 (2015) 3107–3111 https://doi.org/10.1021/acs.jpca.5b00443.
[85] O. Fizer, M. Fizer, V. Sidey, Y. Studenyak, R. Mariychuk, Benchmark of different charges for prediction of the partitioning coefficient through the hydrophilic/lipophilic index, J. Mol. Model. 24 (2018) 141 https://doi.org/10.1007/s00894-018-3692-x.